International Journal of Heat and Mass Transfer 83 (2015) 284–293

Contents lists available at ScienceDirect

International Journal of Heat and Mass Transfer

journal homepage: www.elsevier.com/locate/ijhmt

Experimental study on energy conversion efficiency during static flash of aqueous NaCl solution

Dan Zhang [a], Junjie Yan [a,*], Bingchao Zhao [a], Jiangtao Feng [b]

[a] State Key Laboratory of Multiphase Flow in Power Engineering, School of Energy & Power Engineering, Xi'an Jiaotong University, Xi'an, Shaanxi 710049, PR China
[b] Department of Environmental Science & Engineering, Xi'an Jiaotong University, Xi'an, Shaanxi 710049, PR China

ARTICLE INFO

Article history:
Received 21 April 2014
Received in revised form 21 October 2014
Accepted 2 December 2014
Available online 19 December 2014

Keywords:
Static flash
Aqueous NaCl solution
Energy conversion efficiency
Energy conversion diagram
Steam-carrying effect

ABSTRACT

Energy conversion during static flash of aqueous NaCl solution was newly analyzed with steam-carrying effect taken into consideration. The energy converted into latent heat of flash steam was defined as used energy, and its fraction in total released energy from unit mass of initial waterfilm was defined as energy conversion efficiency (*ECE*), which varied between 0.023 and 0.991 in current experimental range. Results also suggested that, first, *ECE* increased with rising initial temperature of waterfilm or with slowing down flash speed, but it decreased with the increasing of superheat, or initial height, or initial concentration of waterfilm. Third, both *ECE* and the used energy could be improved simultaneously by reducing superheat and at the same time enlarging orifice diameter while keeping other initial parameters unchanged. At last a calculation formula for *ECE* was proposed within acceptable error range.

1. Introduction

Flash defines the phenomenon that superheated liquid quickly evaporates when it is exposed to sudden pressure drop below its saturation pressure. This violent evaporation significantly reduces the temperature of the liquid and quickly generates massive flash steam. In this paper, "flash" just stands for this sudden evaporation from horizontal waterfilm. This kinds of flash can be further classified into circulatory flash or static flash according to whether the waterfilm has horizontal velocity or not. During flash, the waterfilm rolls fiercely and some liquid is entrained away by upward flowing flash steam, which is defined as steam-carrying effect. Thus, static flash is a complex process containing both heat and mass transfer. Heat transfer is caused by evaporation only, while mass transfer is caused by both evaporation and steam-carrying effect. Flash has wide applications, such as energy recycle in geothermal power plant [1], desalination [2], thin film deposition and [3] so on. Therefore it is studied by scholars world-wide.

Miyatake et al. [4,5] studied static flash of pure water through experiment with superheats varying between 3 and 5 K. Results indicated that the temperature of waterfilm dropped quickly at beginning, then slowly and finally equalized at certain value. Therefore, they divided flash into fast evaporation stage and gradual evaporation stage. Further, they also defined the saturation temperature corresponding to final equilibrium pressure of flash chamber as theoretical equilibrium temperature of waterfilm (T_s). Upon this benchmark, they defined non-equilibrium fraction (*NEF*, clearly discussed in Section 3.1.1) to measure and the degree of completion for flash, and suggested that 1-*NEF* could be used to evaluate energy conversion efficiency for flash. Results suggested that higher superheat or lower initial height of waterfilm led flash to take place faster and evaporate more completely. Saury et al. [6] also examined static flash of pure water, but enlarged experimental range of superheat to between 1 and 35 K. Results suggested that the sensible heat released during temperature drop of waterfilm could be considered to all change into the latent heat of flash steam. Saury et al. [7] also examined influence of depressurization rate on evaporation and found that it had nearly nothing to do with final evaporated mass. Kim [8] further examined static flash of pure water and revealed several critical transition points in temperature evolution of waterfilm. Studies on flash of aqueous NaCl solution also turned up mainly for its application in desalination. Gopalakrishna et al. [9] carried out static flash of aqueous NaCl solution. Superheat ranged between 0.5 and 10 K, concentration of NaCl between 0 and 0.035 (mass fraction). According to experimental results, they proposed a formula for final evaporated mass. Lu Liu et al. [10] performed experiments on flash of aqueous NaCl droplet, and found the evaporation rate could be reduced by higher concentration or ambient pressure.

In recent years, our research team also carried out a series of experimental studies on static flash of both pure water [11] and

* Corresponding author. Tel./fax: +86 (29) 8266 5741.
E-mail address: yanjj@mail.xjtu.edu.cn (J. Yan).

http://dx.doi.org/10.1016/j.ijheatmasstransfer.2014.12.012
0017-9310/

Nomenclature

A	cross-section area of flash chamber (m^2)
A_{usd}	area of E_{usd} in energy conversion diagram (–)
c	specific heat (kJ kg^{-1} K^{-1})
D	orifice diameter of throttle plate (mm)
e	error (–)
ECE	energy conversion efficiency (–)
E_{tt}	total released energy from unit mass of initial waterfilm (kJ kg^{-1})
E_{us}	usable energy contained in unit mass of initial waterfilm (kJ kg^{-1})
E_{usd}	used energy contained in unit mass of initial waterfilm (kJ kg^{-1})
f_m	concentration (mass fraction) of aqueous NaCl solution (–)
FS	flash speed (s^{-1})
h	specific enthalpy (kJ kg^{-1})
H	height of waterfilm (m)
h_{fg}	latent heat of vaporization (kJ kg^{-1})
L_{cbu}	can-be-used loss in unit mass of initial waterfilm (kJ kg^{-1})
L_{cnu}	cannot-be-used loss in unit mass of initial waterfilm (kJ kg^{-1})
L_{tt}	total energy loss in unit mass of initial waterfilm (kJ kg^{-1})
m	mass (kg)
NEF	non-equilibrium fraction (–)
p	pressure (MPa)
t	temperature (°C)
u	specific internal energy (kJ kg^{-1})

Greek symbols

θ	boiling point elevation (°C)
ΔH	height drop of waterfilm (m)
ΔT	superheat (K)
ρ	density (kg m^{-3})
τ	time (s)

Subscripts

0	start of flash
B	aqueous NaCl solution (brine)
cal	calculated value
dp	dividing point between fast and gradual evaporation stages
e	equilibrium
exp	experimental
fit	fitting value
im	integral mean
LST	least slope tangent line
max	maximum
r	relative
rf	reference
s	saturated
sc	steam-carrying
stm	steam
tg	tangent point
v	vacuum chamber

aqueous NaCl solution [12]. In our experiments, concentration of waterfilm was enlarged into 0–0.15 (mass fraction), superheat into 1.7–53.9 K. It was found that the temperature evolution of waterfilm in static flash was strongly analogous to that in classical model of semi-infinite body after a temperature disturbance on its surface had been imposed, thus error function was recruited to fit into *NEF* evolution in static flash within acceptable error range. Static flash at different flash speeds was also studied [13]. Flash speed was defined as the mean drop rate of *NEF* during fast evaporation stage (clearly discussed in Section 3.1.1). In experiments, different flash speeds were generated by adding throttle orifice plate with different orifice diameters (5–80 mm) between flash and vacuum chambers. Results suggested that, first, shrinking orifice diameter was an effective way to adjust flash speed. Second, increasing superheat strengthened boiling heat transfer during fast evaporation stage, but the increasing of initial height/concentration of waterfilm or shrinking orifice diameter just did oppositely. It was also found that the height drop of waterfilm measured in experiments was always far greater than the theoretical height drop of waterfilm calculated by heat balance, suggesting that steam-carrying effect was ubiquitous in flash evaporation and the height drop of waterfilm (or mass transfer) was caused by both evaporation and steam-carrying effect [14]. Results further indicated that increasing superheat, or initial height or initial concentration of waterfilm intensified steam-carrying effect and increased height drop of waterfilm, while shrinking orifice diameter greatly suppressed steam-carrying effect and reduced the height drop. In light of force analysis of single droplet submerged in upward flowing steam, a calculation model for steam-carrying effect at different flash speeds was set up [15]. Besides, Our research team also carried out experimental studies on circulatory flash of both pure water and aqueous NaCl solution [16,17] and compared their boiling heat transfer properties with that of static flash [11]. An improvement for custom MSF system was also proposed and analyzed [18].

Former works revealed basic mechanism of heat and mass transfer during flash, but in their analysis, the energy released from superheated waterfilm was considered to all changed into the latent heat of flash steam. The energy loss induced by steam-carrying effect was not considered. With the increasing of superheat or initial concentration of waterfilm, steam-carrying effect was significantly intensified [15] and played a major role in mass transfer, wasting considerable energy that cannot be neglected.

Therefore, this paper re-analyzes the composition of the released energy during flash with steam-carrying effect taken into consideration. The energy converted into latent heat of flash steam is viewed as used energy and its fraction in the total released energy from unit mass of initial waterfilm is defined as energy conversion efficiency (*ECE*). This efficiency is measured through experiment and its dependences on initial parameters are also analyzed with help of energy conversion diagram. At last, a calculation formula for *ECE* is proposed within acceptable error range.

2. Experimental system and uncertainty analysis

2.1. Experimental system

Research in this paper is carried out on base of the same experimental system (Fig. 1) and steps stated in our former works [13,14]. The experimental system contains high and low pressure part. High pressure part contains heater and flash chamber. The flash chamber is a rectangular tank with cross section of 0.20 × 0.20 m and height of 0.50 m. To achieve visualization, its front and rear faces are made of tempered glass, the other 4 faces are made of stainless steel and are finely insulated by thick asbestos layers. Low pressure part includes vacuum chamber, vacuum pump and auxiliary condensing system. Two parts are connected by electromagnetic valve with internal diameter is 80 mm. In order

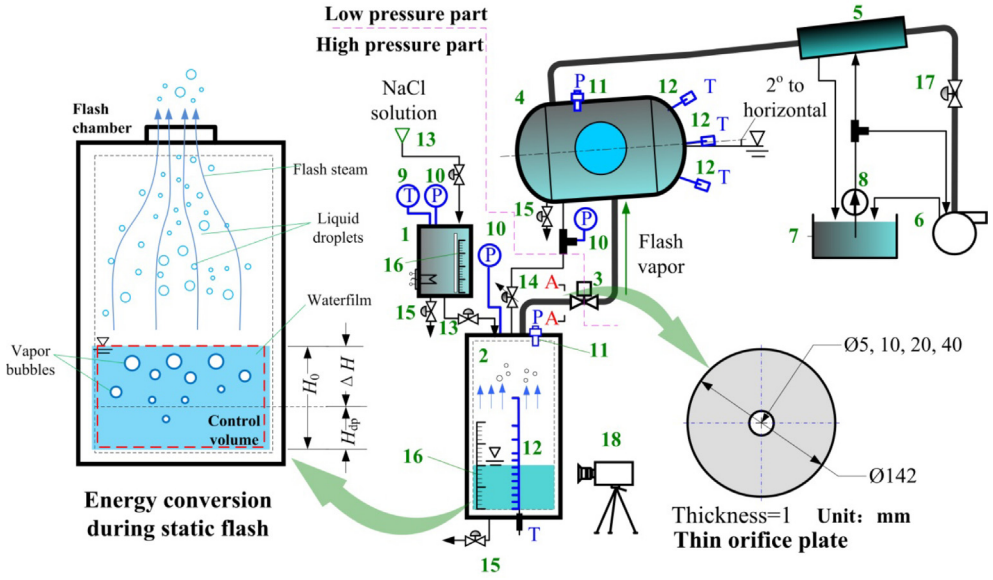

(1). heater
(2). flash chamber
(3). electromagnetic valve
(4). vacuum chamber
(5). condenser
(6). vacuum pump
(7). cooling water tank
(8). cooling water pump
(9). thermometer
(10). barometer
(11). pressure transducer
(12). thermocouples
(13). filling valve
(14). adjusting valve
(15). drain valve
(16). cathetometer
(17). adjusting valve
(18). high speed camera

Fig. 1. Experimental system for static flash of aqueous NaCl solution.

to generate different flash speeds, four thin orifice plates with different orifice diameters (5, 10, 20, 40 mm) are respectively installed at the inlet of electromagnetic valve (section A-A in Fig. 1) to throttle flash steam. Combined with the state without orifice plate, five different flow areas are available. The structure of each component, information of measuring equipments, as well as data processing have been introduced in detail in Ref. [13,14] which are not repeated here.

In trials, aqueous NaCl solution was heated and filled into flash chamber to required level. At the same time, auxiliary condensing system and vacuum pump were turned on to reduced vacuum chamber pressure to designed value. Then, the electromagnetic valve was opened and flash took place suddenly. Meanwhile, temperature of waterfilm, pressure of flash and vacuum chamber were real-timely measured and stored. Initial and final equilibrium height of waterfilm were monitored by a cathetometer attached outside the front glass of flash chamber. After flash, remain liquid was drained out and its concentration was measured by float densimeter.

2.2. Uncertainty analysis

The experimental ranges of main parameters and the uncertainty analysis results for all directly and indirectly measured values are all listed in Table 1. The uncertainty analysis is carried out according to method of *constant odds–product form* proposed by Moffat [19].

3. Result and analysis

3.1. Energy conversion ratio (ECE)

In the energy released during flash, the part changing into the latent heat of flash steam cannot only represent the strength of flash boiling, but can also be utilized in industrial flash system (e.g. multi-stage flash system). Therefore, the latent heat contained in flash steam is defined as used energy in this paper, and energy conversion efficiency (*ECE*) is defined as the fraction of the used

Table 1
Experimental range of main parameters and uncertainty analysis.

Parameter x_x	Experimental range	Absolutely uncertainty δx_x	Minimal measured value x_{xmin}	Maximal uncertainty $\delta x_x/x_{xmin}$
T (°C)	46.5–132.4	0.2	46.5	4.30×10^{-3}
H (m)	0.10, 0.15, 0.20, 0.25, 0.30	5.0×10^{-4}	0.10	0.005
f_m	0, 0.05, 0.10, 0.15	5.0×10^{-4}	0.05[a]	0.010
τ (s)	20–1000	0.0125	20	6.25×10^{-4}
p (MPa)	8.68×10^{-3}–0.213	1.13×10^{-3}	8.68×10^{-3}	0.130
ΔT (K)	2.0–43.8	0.2	2	0.100
NEF	–	–	–	0.100
ECE	–	–	–	0.142

[a] Pure water does not require concentration measurement.

energy in the total released energy from unit mass of initial waterfilm. Its expression is deduced on basis of following concepts.

3.1.1. Basic concepts

Static flash is an unstable boiling, during which temperature of waterfilm drops quickly at first, then slowly and finally equalizes at certain value. Thus, theoretical equilibrium temperature of waterfilm (t_{Bse}) is introduced as Eq. (1) to represent the lowest temperature that waterfilm can reach in theory. In this formula, t_s is saturation temperature of pure water under final equilibrium pressure of flash chamber (p_{fe}) and θ is boiling point elevation of aqueous NaCl solution.

$$t_{Bse} = t_s(p_{fe}) + \theta(t_{Be}, f_{me}) \tag{1}$$

On basis of t_{Bse}, superheat and non-equilibrium fraction (*NEF*) are respectively defined as Eqs. (2) and (3) to represent maximum temperature drop and measure completion degree of flash. Our former works [13] proposes fitting formula for *NEF* as Eq. (4) on basis of experimental results.

$$\Delta T = t_{B0} - t_{Bse} \tag{2}$$

$$NEF(\tau) = \frac{t_B(\tau) - t_{Bse}}{t_{B0} - t_{Bse}} = \frac{t_B(\tau) - t_{Bse}}{\Delta T} \tag{3}$$

$$NEF(\tau) = \mathrm{erf}\left[\left(\frac{H_0}{2}\sqrt{\frac{\rho_B c_B}{\lambda\tau}}\right)^{a_2}\right] \tag{4}$$

where $\lambda = 1.106\left(\frac{\Delta T H_0}{D^2}\right)^{-0.535}\exp(-1.603 f_{m0})$, and $a_2 = 0.0011 + 0.3400\ln\Delta T + 0.0202D - 0.0002D^2$.

As shown in Fig. 2, flash can be divided into fast evaporation stage and gradual evaporation stage [13] due to the distinctly different decreasing rates of *NEF* at the beginning and the end of flash. Ref. [13,15] defines the dividing time (τ_{dp}) of two stages as the intersection of horizontal line *NEF* = 0 and the least slope tangent along curve of *NEF* (point B in Fig. 2), The duration of fast evaporation stage [0, τ_{dp}] is defined as flash duration time. In light of above NEF fitting formula, the dividing time can be computed by Eq. (5) [13].

$$\tau_{dp} = \tau_{tg,LST} - \frac{NEF(\tau_{tg,LST})}{NEF'(\tau_{tg,LST})} \tag{5}$$

where $\tau_{tg,LST} = \left(\frac{\beta-1}{2\alpha^2\beta}\right)^{\frac{1}{2\beta}}$, $\alpha = \left(\frac{H_0}{2}\sqrt{\frac{\rho c_p}{\lambda}}\right)^{a_2}$, $\beta = -\frac{a_2}{2}$, and $NEF'(\tau) = \frac{2}{\sqrt{\pi}}\alpha\beta e^{-\alpha^2\tau^{2\beta}}\tau^{\beta-1}$.

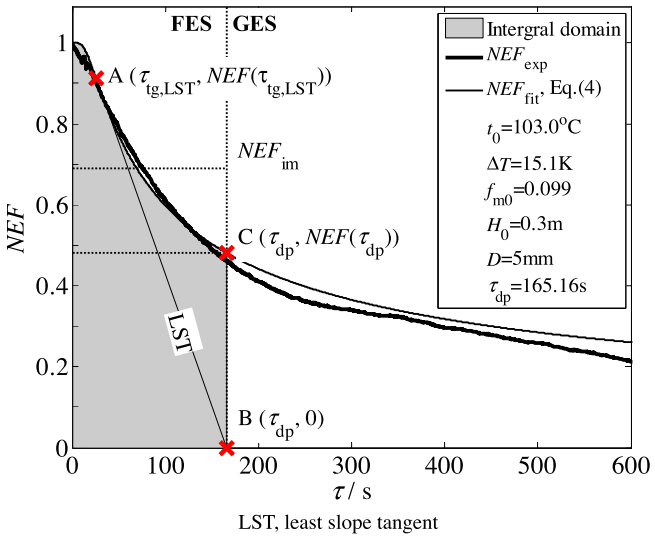

LST, least slope tangent

Fig. 2. Dividing time between fast evaporation stage (FES) and gradual evaporation stage (GES).

NEF represents the completion degree of flash, but it drops nonlinearly with time. In order to measure the overall level of completion speed of flash, flash speed (*FS*) is introduced and defined as mean drop rate of *NEF* during flash duration time [0, τ_{dp}] as Eq. (6) [13]. Considering *NEF* is dimensionless, so the unit of *FS* is "s^{-1}".

$$FS = \frac{1 - NEF_{dp}}{\tau_{dp}} \tag{6}$$

Here and in following calculation, the reference temperature and concentration are respectively defined as Eqs. (7) and (8), according to which thermo-properties data of aqueous NaCl solution are cited from Refs. [20,21].

$$t_{rf} = \frac{1}{2}(t_{B0} + t_{Bse}) \tag{7}$$

$$f_{mrf} = \frac{1}{2}(f_{m0} + f_{me}) \tag{8}$$

3.1.2. Expression of ECE

As shown in Fig. 1, waterfilm is selected as control volume to analyze energy conversion during flash because phase-change takes place within it. The mass transfer during flash is caused by both evaporation and steam-carrying effect according to Ref. [14,15], therefore, mass decrease of waterfilm can be expressed as Eq. (9).

$$-dm_B = dm_{stm} + dm_{sc} \tag{9}$$

If heat loss through wall of flash chamber is neglected, energy balance for this control volume can be expressed as Eq. (10). Further assuming that the liquid and steam keep saturated during flash, the enthalpy of flash steam can be expressed as Eq. (11). Substituting it as well as Eq. (9) into Eq. (10), energy balance is expanded as Eq. (12). In this formula, left side is total released energy in the differential process; first item at right side (behind first equal sign) is the energy that has been used; the second item is the liquid enthalpy still contained within flash steam after its condensation; the third item is the energy that is taken out of control volume by entrained liquid due to steam-carrying effect. Because the second and third items do not take part in phase-change during flash, thus they are combined together (second term behind second equal sign) and viewed as unused energy, or energy loss.

$$0 = d(m_B u_B) + h_{stm}dm_{stm} + h_B dm_{sc} \tag{10}$$

$$h_{stm} = h_B + h_{fg} \tag{11}$$

$$\underbrace{-d(m_B u_B)}_{\substack{\text{total released}\\ \text{energy}}} = \underbrace{h_{fg}dm_{stm}}_{\text{used energy}} + \underbrace{h_B dm_{stm}}_{\substack{\text{liquid enthalpy}\\ \text{contained}\\ \text{in steam}}} + \underbrace{h_B dm_{sc}}_{\substack{\text{energy contained}\\ \text{by be-carried}\\ \text{liquid}}} = \underbrace{h_{fg}dm_{stm}}_{\text{used energy}} - \underbrace{h_B dm_B}_{\substack{\text{unused}\\ \text{energy}}} \tag{12}$$

If choose theoretical equilibrium temperature of waterfilm (t_{Bse}, Eq. (1)) as benchmark to measure energy change and further neglect difference between liquid's specific heat at constant pressure and that at constant volume, specific internal energy and enthalpy of aqueous NaCl solution can be expressed as Eq. (13), by which energy balance Eq. (12) is expanded as Eq. (14). In this formula, the density (ρ_B) and specific heat (c_B) of aqueous NaCl solution, as well as the latent heat (h_{fg}) of steam are function of temperature (t_B) and concentration (f_m) of waterfilm, both of which change during flash. The relative changes of ρ_B, c_B, h_{fg} in each flash are computed and their variation ranges in current experiment are listed in Table 2. It suggests that the relative variations of the three properties during flash are no more than 5% and therefore can be

Table 2
Relative variation of thermo-properties during flash in current experimental range.

Thermo-properties	Relative variation
$\frac{\rho_{Bdp}-\rho_{B0}}{\rho_{B0}}$	$1.23\times10^{-4}-0.033$
$\frac{c_{Bdp}-c_{B0}}{c_{B0}}$	-0.026–0.044
$\frac{h_{fg,dp}-h_{fg,0}}{h_{fg,0}}$	$2.32\times10^{-4}-0.047$

approximately viewed as constant. Their values are also cited from Refs. [20,21] through reference temperature and concentration defined as Eqs. (7) and (8).

$$u = h = c_B(t_B - t_{Bse}) \tag{13}$$

$$-d[\rho_B AHc_B(t_B - t_{Bse})] = h_{fg}dm_{stm} - c_B(t_B - t_{Bse})d(\rho_B AH) \tag{14}$$

Now that thermo-properties are independent of temperature, the energy conversion during entire flash duration time can be deduced as Eq. (15) by integral Eq. (14) during $[0, \tau_{dp}]$. Average its both sides into the mass of initial waterfilm (Eq. (16)), Eq. (17) is reached. Then, energy conversion efficiency (*ECE*) can be expressed as Eq. (18).

$$\rho_B Ac_B[H_0(t_{B0} - t_{Bse}) - H_{dp}(t_{Bdp} - t_{Bse})] = h_{fg}m_{stm} - \rho_B Ac_B\int_0^{\tau_{dp}}[t_B(\tau) - t_{Bse}]dH \tag{15}$$

$$m_0 = \rho_B AH_0 \tag{16}$$

$$c_B[(t_{B0} - t_{Bse}) - H_{dpr}(t_{Bdp} - t_{Bse})] = \frac{h_{fg}m_{stm}}{\rho_B AH_0} - c_B\int_0^{\tau_{dp}}[t_B(\tau) - t_{Bse}]dH_r \tag{17}$$

where $H_r = \frac{H}{H_0}$.

$$ECE = 1 - \frac{-\int_0^{\tau_{dp}}[t_B(\tau) - t_{Bse}]dH_r}{(t_{B0} - t_{Bse}) - H_{dpr}(t_{Bdp} - t_{Bse})} = 1 - \frac{-\int_0^{\tau_{dp}}[t_B(\tau) - t_{Bse}]\frac{dH_r}{d\tau}d\tau}{(t_{B0} - t_{Bse}) - H_{dpr}(t_{Bdp} - t_{Bse})} \tag{18}$$

In experiments, t_B is real-timely measured, but the height of waterfilm cannot be. Fig. 3 displays photo of flash taken by high speed camera and suggests that flash steam has no time to diffuse out of waterfilm during flash, but fully blends with liquid to form foam-like mixture, expanding upward in flash chamber at first and then falling back. The height of waterfilm (liquid height) cannot be measured until flash steam completely diffuses out and waterfilm returns equilibrium after flash. Therefore, the instantaneous variation rate of the relative height of waterfilm ($dH_r/d\tau$) in Eq. (18) has to be approximately replaced by its mean drop rate during $[0, \tau_{dp}]$ as Eq. (19). Substituting it as well as *NEF*'s definition (Eq. (3)) into Eq. (18), *ECE* is greatly simplified as Eq. (20) in which NEF_{im} is the integral mean value of *NEF*. In following discussion, subscript "im" stands for the integral average of variable during $[0, \tau_{dp}]$.

$$\frac{dH_r}{d\tau} \approx -\frac{\Delta H_r}{\tau_{dp}} \tag{19}$$

$$ECE = 1 - \frac{-\int_0^{\tau_{dp}} NEF\cdot dH_r}{1 - H_{dpr}NEF_{dp}} \approx 1 - \frac{\Delta H_r\frac{1}{\tau_{dp}}\int_0^{\tau_{dp}} NEF\cdot d\tau}{1-(1-\Delta H_r)\cdot NEF_{dp}} = 1 - \frac{\Delta H_r\cdot NEF_{im}}{1 - NEF_{dp} + \Delta H_r NEF_{dp}} \tag{20}$$

where $NEF_{im} = \frac{1}{\tau_{dp}}\int_0^{\tau_{dp}} NEF\cdot d\tau$

In Eq. (20), the relative height drop of waterfilm (ΔH_r) reflects the strength of mass transfer during flash. While NEF_{dp} reflects the strength of boiling heat transfer because boiling or evaporation is the only reason leads *NEF* to reduce. NEF_{im} reflects the decay process of boiling intensity. Eq. (20) indicates that *ECE* depends not only on the relative strength between heat and mass transfer during flash, but also on the specific decaying process of heat transfer intensity. In other words, it cannot evaluate energy conversion efficiency by *NEF* only.

In this paper, Eq. (20) is used as measurement formula for *ECE*. Based upon experimental data, *ECE* varies between 0.023 and 0.991 in current range. Besides, our former works [14,15] set up calculation model for steam-carrying effect and proposes calculation formula for height drop of waterfilm as Eq. (21). Combined with above fitting formula for *NEF* (Eq. (4)), *ECE* can also be directly calculated by Eq. (22).

$$\Delta H_{cal} = H_0\cdot\frac{c_B\Delta T}{h_{fg}}\cdot(1 - NEF_{dp})\left[1 + C\cdot\frac{\rho_B^4}{\rho_{stm}^3}\cdot\left(H_0\cdot\frac{c_B\Delta T}{h_{fg}}\cdot FS\right)^6\right] \tag{21}$$

where $\ln C = b_1 + b_2\Delta T - 27.6204\exp(-\Delta T^{0.5}) + 10.3227\ln H_0 + 13.287 f_{m0}$, and $b_1 = 0.002D^2 - 0.5043D + 62.083$, b_2 is listed in Table 1 of Ref. [15].

$$ECE_{cal} = 1 - \frac{\Delta H_{calr}\cdot NEF_{im}}{1 - (1 - \Delta H_{calr})\cdot NEF_{dp}} \tag{22}$$

where $\Delta H_{calr} = \frac{\Delta H_{cal}}{H_0}$.

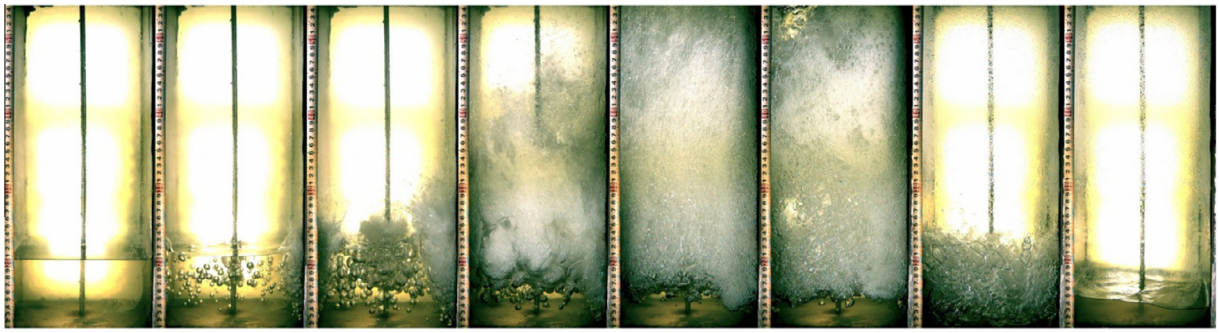

Fig. 3. Flash process photos taken by high-speed camera.

3.1.3. Energy conversion diagram

Fig. 4 displays evolution of *NEF* versus relative height of waterfilm (H_r). During flash, both *NEF* and H_r decrease from 1 at start point O to NEF_{dp} and H_{dpr} respectively at finishing point G. Besides, this figure also displays the composition of released energy from unit mass of initial waterfilm by reshaping *ECE* (expression behind first equal sign in Eq. (20)) as Eq. (23).

$$ECE = 1 - \frac{\underbrace{-\int_0^{\tau_{dp}} NEF \cdot dH_r}_{L_{tt},\text{total energy loss}}}{\underbrace{1 - H_{dpr}NEF_{dp}}_{E_{tt},\ \text{total released energy}}} = 1 - \frac{\underbrace{-\int_0^{\tau_{dp}} (NEF - NEF_{dp}) \cdot dH_r}_{L_{cbu},\ \text{loss contains usable energy}} + \underbrace{\Delta H_r \cdot NEF_{dp}}_{L_{cnu},\ \text{loss cannot be used}}}{\underbrace{(1 - NEF_{dp})}_{E_{us},\ \text{energy can be used}} + \underbrace{\Delta H_r \cdot NEF_{dp}}_{L_{cnu},\ \text{loss cannot be used}}} \tag{23}$$

The denominator in Eq. (23) equals to the area OBCGEFO in Fig. 4, which represents total released energy (E_{tt}) from unit mass of initial waterfilm during flash. E_{tt} contains 3 parts, such as ABCGA, OAGO and OGEFO.

Part ABCGA equals to second term in numerator (or denominator) behind second equal sign in Eq. (23). It represents the proportion below temperature of waterfilm at finishing point (t_{Bdp}) in the energy taken away by mass transfer (includes flash steam and entrained liquid). Thus, this part of energy cannot be used during flash and is named as cannot-be-used loss (L_{cnu}). While part OAGO equals to the first term in numerator behind second equal sign. It reflects the proportion above t_{Bdp} in the energy taken away by mass transfer. Thus OAGO represents the usable energy that can be used but has not been used during flash, and is named as can-be-used loss (L_{cbu}). The sum of L_{cnu} and L_{cbu} (OBCGO) equals to the numerator behind first equal sign and they make up the total energy loss (L_{tt}) during flash.

Except L_{tt}, the remain part of E_{tt} (OGEFO) represents the energy changed into latent heat of flash steam, or the used energy (E_{usd}) in unit mass of initial waterfilm. The sum of L_{cbu} and E_{usd} (OAEF) equals to first term in denominator behind second equal sign and represents the maximum usable energy (E_{us}) during flash.

In brief, E_{tt} in flash converts into three parts, such as E_{usd}, L_{cbu} and L_{cnu}. Among them, E_{tt} and L_{cnu} depend only on the location of finishing point, but E_{usd}, L_{cbu} also depend on specific evolution process of *NEF* versus H_r (shape of curve OG) during flash. Therefore, figure of *NEF*-H_r is recruited as energy conversion diagram for flash.

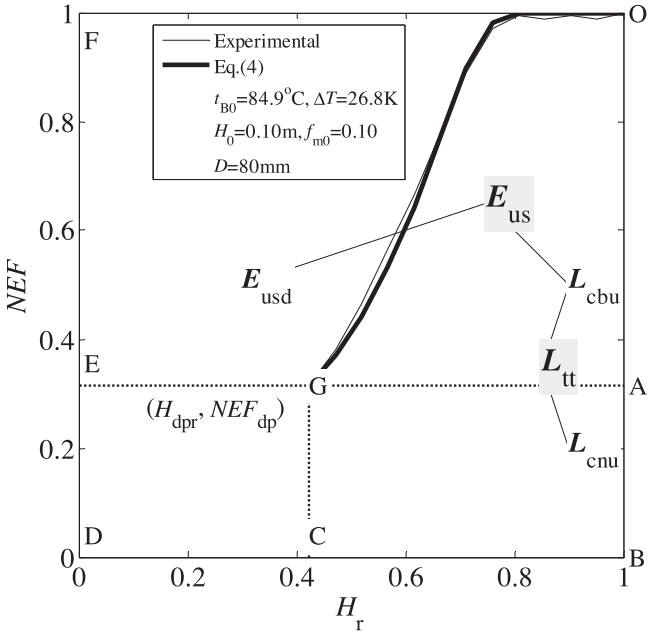

Fig. 4. Energy conversion diagram.

3.2. Dependence of ECE on initial parameters

Changing of initial parameters, such as initial temperature of waterfilm, superheat, initial concentration of waterfilm, initial height of waterfilm, as well as orifice diameter, will influence *ECE* through changing the location of G and shape of curve OG in energy conversion diagram, with which their detail influences are discussed as below.

3.2.1. Dependences on superheat and orifice diameter

Fig. 5 displays *ECE* versus superheat under different orifice diameters (D). It suggests that *ECE* decreases with rising superheat. Because our former works [13,15] concludes that increasing superheat does not only reduce NEF_{dp}, but also increases ΔH_r, or reduces H_{dpr} through strengthening both evaporation and steam-carrying effect. Taking D = 80 mm in Fig. 5 for example, when superheat is increased from 15 to 30 K (from G1 to G2 in Fig. 5), NEF_{dp} drops only from 0.285 to 0.280, but ΔH_{dp} greatly increases from 0.2093 to 0.6305. So as shown in energy conversion diagram Fig. 6, increasing superheat moves finishing point lower leftward from G1 to G2, which definitely increases total released energy (E_{tt}). But at same time, the drop speed of *NEF* with reducing H_r becomes more slowly, which makes area OBC2G2O is larger than OBC1G1O, therefore increases the total energy loss (L_{tt}). According to Eq. (20), above variations increase NEF_{im} from 0.741 to 0.748, making L_{tt} increase 203%, but E_{tt} only increase 15.8%, so eventually leads *ECE* to reduce. This result indicates that although increasing superheat strengthens evaporation, the strengthening effect is weaker than that on steam-carrying effect, leading the majority of the increment of total released energy to be directly wasted by strengthened mass transfer without taking part in boiling heat transfer.

Fig. 5 also displays that, under same superheat, *ECE* significantly increases with decreasing D when it is shrunk from 80 to 20 mm, but the increment becomes unobviously when it is further shrunk from 10 to 5 mm. This result could also be explained with the help of Fig. 6. Previous works [13] suggest that shrinking D increases NEF_{dp}, and at the same time significantly reduces relative height drop of waterfilm by suppressing steam-carrying effect. Taking ΔT = 15 K in Fig. 5 for example, shrinking D from 80 to 20 mm

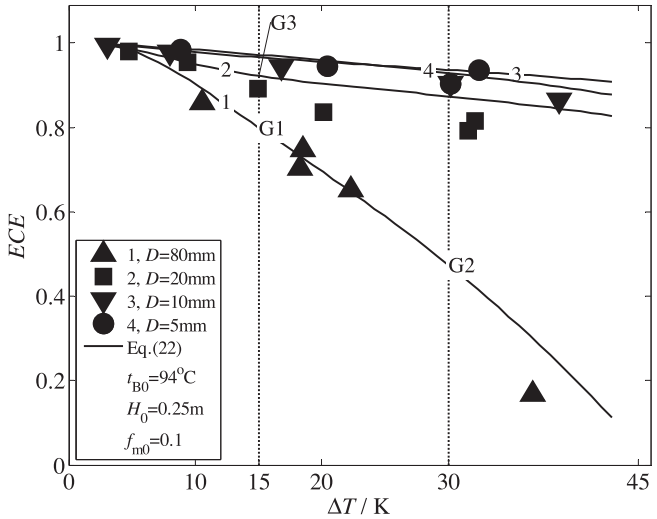

Fig. 5. *ECE* versus superheat under different orifice diameters.

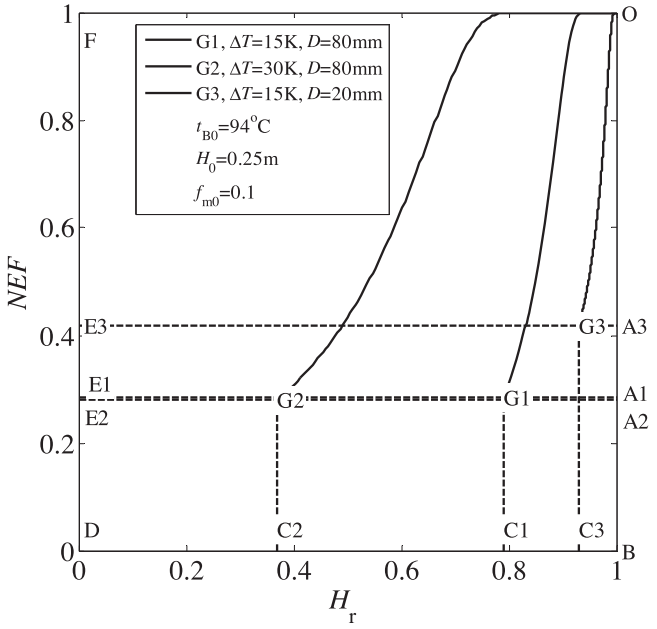

Fig. 6. Influences of increasing superheat or shrinking orifice diameter on energy conversion diagram.

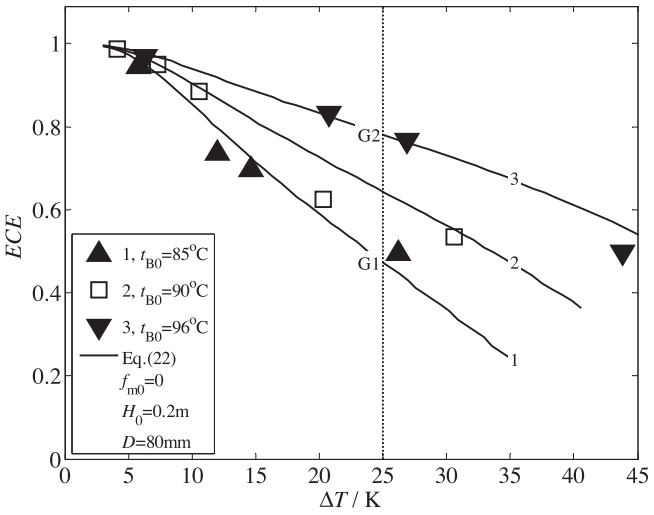

Fig. 7. *ECE* versus superheat under different initial temperatures of waterfilm.

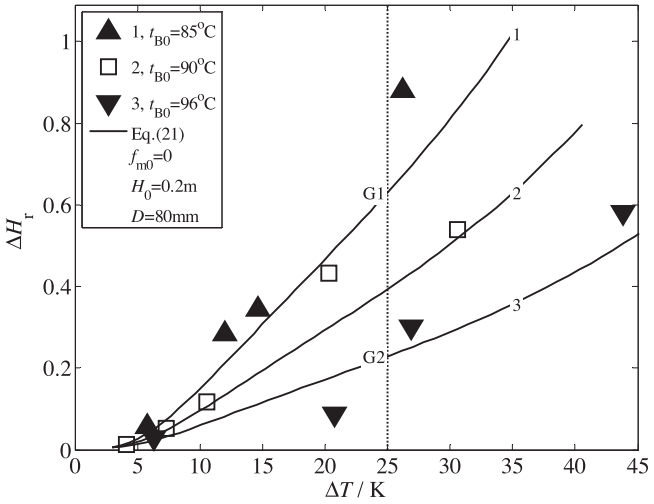

Fig. 8. Relative height drop of waterfilm versus superheat under different initial temperatures of waterfilm.

(G1 to G3) leads NEF_{dp} to increase from 0.285 to 0.418, leads H_r to significantly increase from 0.791 to 0.930, and therefore makes finishing point in energy conversion diagram move upper rightward from G1 to G3, which definitely reduces total released energy (E_{tt}). But at the same time, the drop of *NEF* versus reducing H_r becomes steeper, leading the area of total energy loss (L_{tt}) also to shrink from OBC1G1O to OBC3G3O. According to Eq. (20), above variation reduces L_{tt} and E_{tt} respectively for 69.4% and 21.1%, thus makes *ECE* eventually increase, but at the same time reduces the used energy (E_{usd}) for 9%. When *D* is further reduced, the increment of NEF_{dp} and H_r is unobvious. Also taking $\Delta T = 15$ K in Fig. 5 for example, when *D* is reduced from 10 to 5 mm, NEF_{dp} only increases from 0.459 to 0.482 and H_r only increases from 0.972 to 0.978, which makes the finishing point as well as shape of curve OG have no obvious variation, and therefore makes *ECE* nearly does not change. In other words, it is at the cost of reducing used energy that shrinking orifice diameter improves *ECE*, but the improvement becomes weaker when orifice diameter is further shrunk smaller.

Our former works concludes that variation of flash speed mainly depends on orifice diameter [13]. Shrinking orifice diameter reduces flash speed more significantly than adjusting any other initial parameters. Therefore, above result can be also expressed as that, slowing down flash speed by shrinking orifice diameter improves energy conversion efficiency.

3.2.2. Dependence on initial temperature of waterfilm

Fig. 7 displays *ECE* versus superheat under different initial temperatures of waterfilm (t_{B0}). It suggests that *ECE* increases with rising t_{B0} under same superheat.

Because increasing t_{B0} reduces ρ_B/ρ_{stm}, and according to the model of steam-carrying effect [15], this reduction minimizes mean steam speed during flash, which is viewed as the driving force for steam-carrying effect. Therefore increasing t_{B0} eventually leads relative height drop of waterfilm to decrease. This is testified by experimental result shown in Fig. 8 and matches well with calculated result of Eq. (21).

Taking $\Delta T = 25$ K in Fig. 7 for example, after increasing t_{B0} from 85 to 96 °C (G1 to G2), ΔH_r drops from 0.631 to 0.228. Combined with previous conclusion that t_{B0} has nearly no influence on NEF_{dp}, the finishing point in energy conversion diagram (Fig. 9) moves horizontally rightward from G1 to G2. Evidently, area of usable energy does not change, but that of total released energy (E_{tt}) decreases for G2C2C1G1G2. While the area of total energy loss (L_{tt}) decreases for area of OG2C2C1G1O, which is far larger than the reduction of E_{tt}, therefore, finally making both *ECE* and E_{usd} increase. This result indicates that it is through greatly suppressing steam-carrying effect that rising initial temperature of waterfilm utilizes more usable energy and improves *ECE*.

3.2.3. Dependences on initial concentration/height of waterfilm

Fig. 10 displays that *ECE* slightly decreases with increasing initial concentration of waterfilm (f_{m0}). Previous works [13,15] concludes that NEF_{dp} is almost independent on f_{m0}, but rising f_{m0} increases relative height drop of waterfilm (ΔH_r) through strengthening steam-carrying effect. Taking $H_0 = 0.1$ m in Fig. 10 for example, rising f_{m0} from 0 to 0.1 (G1 to G2) increases ΔH_r from 0.234 to 0.255, and moves the finishing point in energy conversion diagram (Fig. 11) horizontally leftward from G1 to G2. This variation does not change the area of total usable energy (E_{us}, OAEF), but enlarges the area of total released energy (E_{tt}) for G1C1C2G2, which is smaller than the increment of the total energy loss (L_{tt}) that equals to

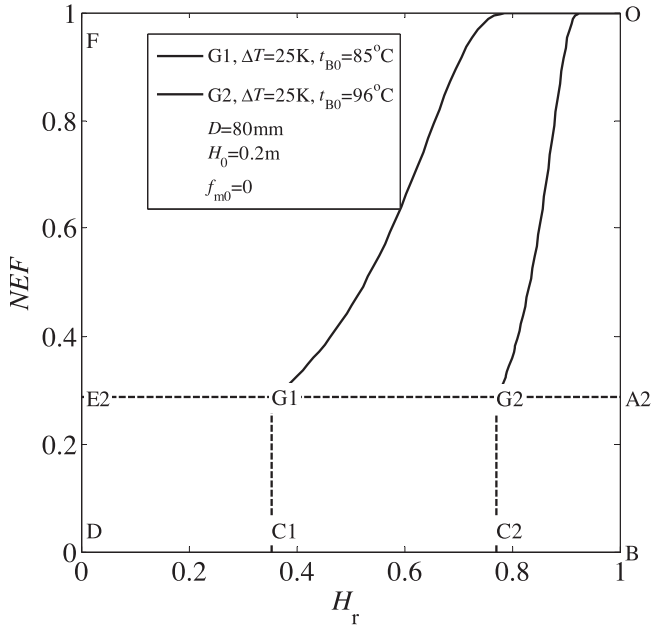

Fig. 9. Influence of increasing initial height of waterfilm on energy conversion diagram.

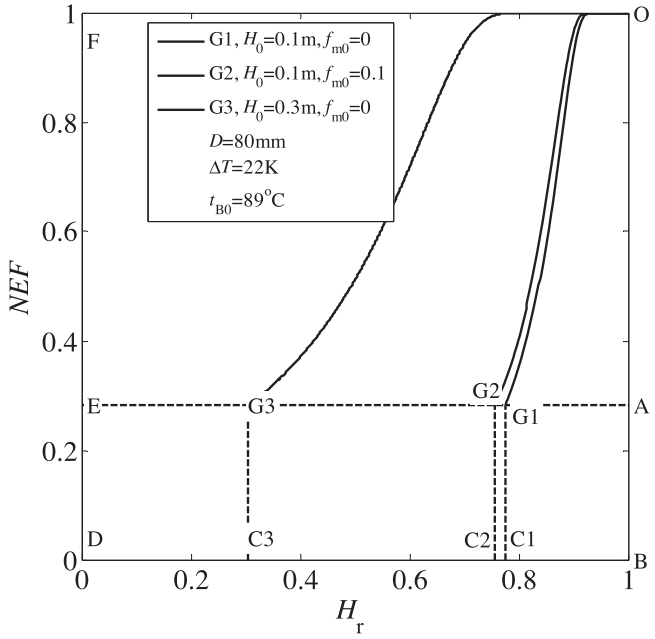

Fig. 11. Influence of increasing initial height of waterfilm or concentration on energy conversion diagram.

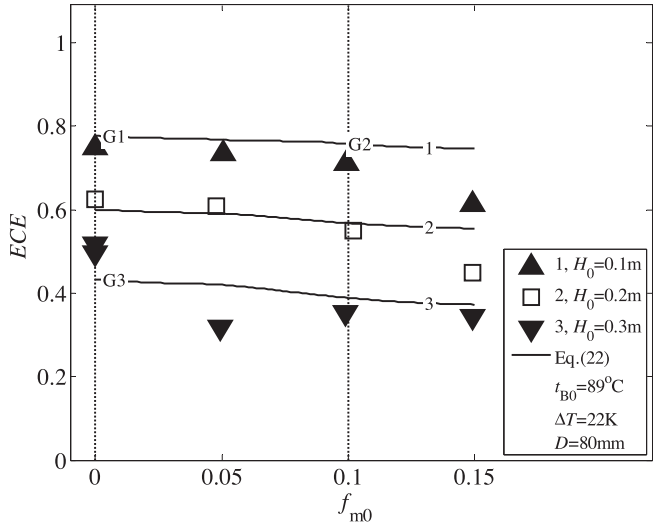

Fig. 10. ECE versus initial concentration of waterfilm under different initial heights of waterfilm.

OG1C1C2G2O, therefore eventually reduces both *ECE* and used energy (E_{usd}, shrinks from OG1EFO to OG2EFO).

Fig. 10 also suggests that under same f_{m0}, *ECE* drops with rising initial height of waterfilm (H_0). Previous works find that rising H_0 cannot only increases relative height drop of waterfilm (ΔH) through strengthening steam-carrying effect, but can also rising NEF_{dp}. Taking $f_{m0} = 0$ in Fig. 10 for example, rising H_0 from 0.1 to 0.3 m raises NEF_{dp} from 0.280 to 0.282, but the increment is negligible compared with the rising of ΔH_r from 0.234 to 0.695. So in energy conversion diagram, finishing point can also be considered to move horizontally leftward from G1 to G3. Similarly as that of increasing f_{m0}, this motion increases L_{tt} much more than that of E_{tt}, leading both *ECE* and E_{usd} to reduce.

These results indicate that rising initial height or initial concentration of waterfilm does not enlarge total usable energy, but wastes a lot of can-be-used energy through strengthening mass transfer.

Besides, solid lines in above Figs. 5, 7 and 10 suggest that calculated *ECE* matches well with experimental result. Fig. 12 further displays that 93% of the relative errors between calculated and experimental *ECE* in current experimental ranges fall in the range of ±30%.

3.3. Improvement of ECE and quantity of used energy

Except of *ECE*, the quantity of used energy from unit mass of initial waterfilm (E_{usd}) is also an important indicator for industrial

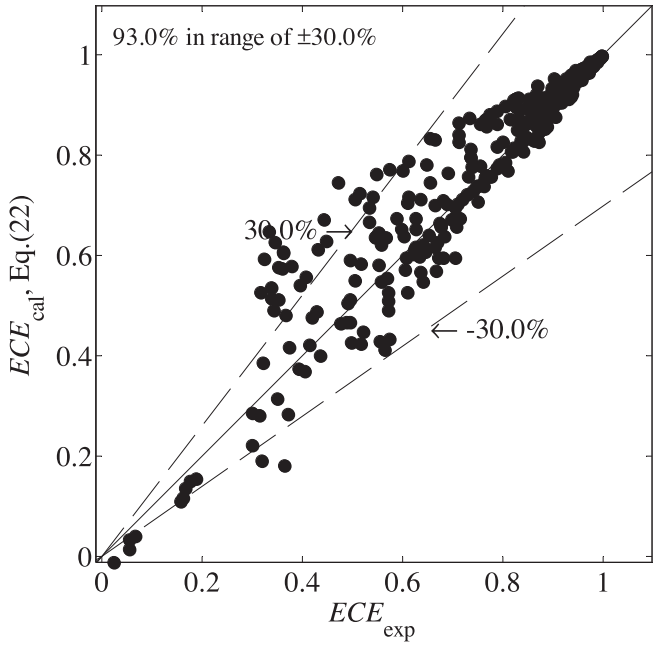

Fig. 12. Relative error between calculated and experimental *ECE* in current experimental range.

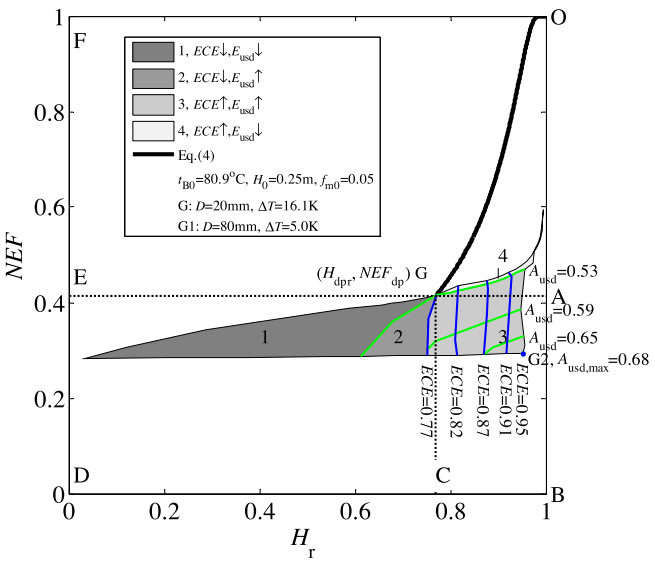

Fig. 13. Variation of *ECE* and E_{usd} by changing superheat and orifice diameter.

flash system. Above discussion suggests that the variations of *ECE* and E_{usd} by adjusting initial parameters does not always change in the same direction. The way to improve both *ECE* and E_{usd} can also be analyzed with help of Eq. (4), Eq. (21) and following Eq. (24), which expresses the area of E_{usd} in energy conversion diagram (OGEFO). A_{usd} is a dimensionless variable, because both the horizontal and vertical coordinates of energy conversion diagram are dimensionless.

$$A_{usd} = ECE_{cal}[1 - (1 - \Delta H_{calr}) \cdot NEF_{dp}] \tag{24}$$

Fig. 13 displays the energy conversion diagram of a flash. If keep its initial temperature (t_{B0}), initial height (H_0) and initial concentration (f_{m0}) of waterfilm as constant, only adjust superheat during 5–32 K and orifice diameter during 5–80 mm (within current experimental range), its finishing point G would change within the shaded area. This shaded area can be divided into part 1–4. E_{usd} will increases if finish point G falls into part 2 and 3, while *ECE* will increases if finishing point G falls into part 3 and 4. The intersection area part 3 is the ideal range where both *ECE* and E_{usd} would increase. Contours for E_{usd} and *ECE* in part 3 further indicate that *ECE* increases with finishing point moving nearly horizontally rightward, while A_{usd} (or E_{usd}) increases with finishing point moving lower rightward. Thus, lower rightmost vertex G2 is the most ideal finishing point for flash with both maximum E_{usd} and *ECE*. It can be reached by reducing superheat from 16.1 K at G to 5 K at G1, and at the same time enlarging orifice diameter from 20 to 80 mm. This result suggests that *ECE* and E_{usd} can be improved simultaneously by reducing superheat and enlarging orifice diameter while keeping other initial parameters unchanged.

4. Conclusion

Experimental study on energy conversion efficiency during static flash of aqueous NaCl solution was carried out on basis of experimental system introduced in our former works [13,14]. The experimental range of main parameters were listed in Table 1.

Figure of *NEF* evolution versus relative height of waterfilm (H_r) as Fig. 4 displayed the conversion of released energy (E_{tt}) from unit mass of initial waterfilm during flash and thus was recruited as energy conversion diagram. This diagram suggested that E_{tt} converted into three parts during flash, such as used energy (E_{usd}, the energy converted into the latent heat of flash steam), can-be-used energy loss (L_{cbu}), and cannot-be-used energy loss (L_{cnb}). The first two made up total usable energy (E_{us}), while the last two made up the total energy loss (L_{tt}). The value of E_{tt} and L_{cnu} depended only on the temperature drop and height drop of waterfilm during flash, but E_{usd}, L_{cbu} also depended on the specific decaying process of temperature/height of waterfilm during flash.

The fraction of E_{usd} in E_{tt} is defined as energy conversion efficiency (*ECE*). Its measurement formula was deduced as Eq. (20) according to the first law of thermodynamics. In current experimental range, *ECE* varied between 0.023 and 0.991.

There were 5 initial parameters whose influences on *ECE* were analyzed, including initial temperature (t_{B0}), initial height (H_0), initial concentration (f_{m0}) of waterfilm, superheat (ΔT) as well as orifice diameter (D) of throttle plate. Results suggested that, first, increasing ΔT moved the finishing point of flash lower leftward in energy conversion diagram, enlarging E_{tt} but reducing *ECE*. Oppositely, slowing down flash speed (*FS*) by shrinking D moved the finishing point upper rightward, reducing E_{tt} but enhancing *ECE*. Second, adjusting t_{B0}, or H_0, or f_{m0} made the finishing point move horizontally in energy conversion diagram, thus did not change quantity of E_{us}. Specifically, increasing t_{B0} moved the finishing point rightward horizontally, and thus increased both E_{usd} and *ECE*. Oppositely, increasing H_0 or f_{m0} moved the fishing point leftward horizontally and reduced both E_{usd} and *ECE*. Third, the change of E_{usd} and *ECE* were not always in the same direction, but they could be simultaneously improved by reducing superheat and at the same time enlarging orifice diameter while keeping other initial parameters unchanged.

At last, on basis of fitting formula for *NEF* (Eq. (4)) and calculation formula for height drop of waterfilm (Eq. (21)) suggested in our former works [13,15], a calculation formula for *ECE* was proposed within acceptable error range.

This paper studies energy conversion on basis of the first law of thermodynamics. Entropy analysis for static flash of aqueous NaCl solution on basis of the second law of thermodynamics is under way now.

Conflict of interest

Neither the entire paper nor any part of its content has been published or has been accepted elsewhere. Also, it is not being submitted to any other journal. We will appreciate your favorable consideration.

Acknowledgments

This work is supported by National Natural Science Foundation of China (51306148/51125027) and the Fundamental Research Funds for the Central Universities.

References

[1] H. Shokouhmand, P. Atashkadi, Performance improvement of a single, flashing, binary, combined cycle for geothermal power plants, Energy 22 (7) (1997) 637–643.
[2] D.H. Kim, A review of desalting process techniques and economic analysis of the recovery of salts from retentates, Desalination 270 (2011) 1–8.
[3] X.K. Duan, Y.Z. Jiang, Microstructure and thermoelectric properties of Sn-doped Bi2Te2.7Se0.3 thin films deposited by flash evaporation method, Thin Solid Films 519 (2011) 3007–3010.
[4] Miyatake, K. Murakami, Y. Kawata, et al., Fundamental experiments with flash evaporation, Heat Transfer – Jpn. Res. 2 (4) (1973) 89–100.
[5] Miyatake, T. Fujii, T. Tanaka, et al., Flash evaporation phenomena of pool water, Heat Transfer – Jpn. Res. 6 (2) (1977) 13–24.
[6] D. Saury, S. Harmand, M. Siroux, Experimental study of flash evaporation of a water film, Int. J. Heat Mass Transfer 45 (16) (2002) 3447–3457.
[7] D. Saury, S. Harmand, M. Siroux, Flash evaporation from a water pool: influence of the liquid height and of the depressurization rate, Int. J. Heat Mass Transfer 44 (2005) 953–965.

[8] J.L. Kim, N. Lior, Some critical transitions in pool flash evaporation, Int. J. Heat Mass Transfer 40 (10) (1997) 2363–2372.
[9] G. Gopalakrishna, V.M. Purushothaman, N. Lior, An experimental study of flash evaporation from liquid pools, Desalination 65 (1987) 139–151.
[10] Lu Liu, Qincheng Bi, Huixiong Li, Experimental investigation on flash evaporation of saltwater droplets released into vacuum, Microgravity Sci. Technol. 21 (Suppl 1) (2009) S255–S260.
[11] Yan Junjie, Zhang Dan, Chong Daotong, et al., Experimental study on static/circulatory flash evaporation, Int. J. Heat Mass Transfer 53 (2010) 5528–5535.
[12] Zhang Dan, Chong Daotong, Yan Junjie, et al., Experimental study on static flash evaporation of aqueous NaCl solution, Int. J. Heat Mass Transfer 55 (23–24) (2012) 7199–7206.
[13] Dan Zhang, Daotong Chong, Junjie Yan, et al., Experimental study on static flash evaporation of aqueous NaCl solution at different flash speeds: heat transfer characteristics, Int. J. Heat Mass Transfer 65 (2013) 584–591.
[14] Zhang Dan, Chong Daotong, Yan Junjie, et al., Study on steam-carrying effect in static flash evaporation, Int. J. Heat Mass Transfer 55 (2012) 4487–4497.
[15] Dan Zhang, Bingchao Zhao, Junjie Yan, et al., Experimental study on static flash of aqueous NaCl solution at different flash speeds: steam-carrying effect, Int. J. Heat Mass Transfer 79 (2014) 618–627.
[16] Yousen Zhang, Jinshi Wang, Junjie Yan, et al., Experimental study on non-equilibrium fraction of NaCl solution circulatory flash evaporation, Desalination 335 (2014) 9–16.
[17] Yousen Zhang, Jinshi Wang, Jiping Liu, et al., Experimental study on heat transfer characteristics of circulatory flash evaporation, Int. J. Heat Mass Transfer 67 (2013) 836–842.
[18] Yan Junjie, Shao Shufeng, Wang Jinhua, et al., Improvement of a multi-stage flash seawater desalination system for cogeneration power plants, Desalination 217 (2007) 191–202.
[19] R.J. Moffat, Contributions to the theory of single-sample uncertainty analysis, J. Fluid Eng. 104 (1982) 250–260.
[20] E. Colin, W. Clarke, D.N. Glew, Evaluation of the thermodynamic function for aqueous sodium chloride from equilibrium and calorimetric measurements below 154 & #xB0;C, J. Phys. Chem. Ref. Data 14 (2) (1985) 489–610.
[21] K.S. Pitzer, J.C. Peiper, R.H. Busey, Thermodynamic properties of aqueous sodium chloride solutions, J. Phys. Chem. Ref. Data 13 (1) (1984) 1–102.